





Crowding tunes the organization and mechanics of actin bundles formed by crosslinking proteins

Jinho Park^{1,2}, Myeongsang Lee^{1,*}, Briana Lee¹ , Nicholas Castaneda^{1,3}, Laurene Tetard^{1,4} and Ellen Hyeran Kang^{1,2,4}

- 1 NanoScience Technology Center, University of Central Florida, Orlando, FL, USA
- 2 Department of Materials Science and Engineering, University of Central Florida, Orlando, FL, USA
- 3 Burnett School of Biomedical Sciences, University of Central Florida, Orlando, FL, USA
- 4 Department of Physics, University of Central Florida, Orlando, FL, USA

Correspondence

E. H. Kang, NanoScience Technology Center, University of Central Florida, 12424 Research Parkway, Orlando, FL 32826, USA Tel: +1 407 823 2368 E-mail: ellen.kang@ucf.edu

Present address

* Department of Physics and Astronomy, Clemson University, Clemson, SC, USA

(Received 20 April 2020, revised 14 September 2020, accepted 21 September 2020, available online 21 October 2020)

doi:10.1002/1873-3468.13949

Edited by Naoko Mizuno

Fascin and α -actinin form higher-ordered actin bundles that mediate numerous cellular processes including cell morphogenesis and movement. While it is understood crosslinked bundle formation occurs in crowded cytoplasm, how crowding affects the bundling activities of the two crosslinking proteins is not known. Here, we demonstrate how solution crowding modulates the organization and mechanical properties of fascin- and α -actinin-induced bundles, utilizing total internal reflection fluorescence and atomic force microscopy imaging. Molecular dynamics simulations support the inference that crowding reduces binding interaction between actin filaments and fascin or the calponin homology 1 domain of α -actinin evidenced by interaction energy and hydrogen bonding analysis. Based on our findings, we suggest a mechanism of crosslinked actin bundle assembly and mechanics in crowded intracellular environments.

Keywords: actin–crosslinking proteins; bending stiffness; binding interaction; bundle organization; macromolecular crowding

Dynamic assembly of actin into higher order structures plays critical roles in intracellular transport, cell shape changes, cell division, movement, and mechanosensing [1–8]. Actin bundles constitute an essential cytoskeletal component present in filopodia [9–12], stress fibers [5,13,14], stereocilia [15], and sensory bristles [15–17]. The mechanical properties of actin bundles largely depend on their architecture, which in turn influence numerous cell functions as well as physiology [8,18].

In living cells, a large number of actin-crosslinking proteins mediate bundle formation with diverse mechanical and structural properties [19–22].

Furthermore, the geometries of crosslinkers have been shown to impact bundle organizations [23,24]. Fascin is a monomeric actin-crosslinking protein (MW = 55 kDa) consisting of two actin-binding sites ~ 5 nm apart [25]. Fascin induces closely packed bundles of parallel filaments modulating cell protrusion and motility [25–29]. Fascin is specifically localized along filopodia [28], thin finger-like structures that play a key role in guided cell movement [30]. Fascin-induced bundles are stiffer than single actin filaments (F-actin), supporting their important role in filopodia extension and force generation [20,31]. Meanwhile, α-actinin is a

Abbreviations

AFM, atomic force microscopy; APTES, (3-aminopropyl)triethoxysilane; ATP, adenosine triphosphate; CH, calponin homology; cryo-EM, cryo-electron microscopy; D, diameter; E_B , Young's modulus; EGTA, ethylene glycol-bis(β -aminoethylether)-N, N, N-tetraacetic acid; FF, force field; FWHM, full width at half maximum; L, length; L_p , persistence length; MD, molecular dynamics; MW, molecular weight; PDB, Protein Data Bank; PEG, polyethylene glycol; R_g , radius of gyration; RMSD, root-mean-square displacement; TIRF, total internal reflection fluorescence; VMD, visual molecular dynamics; κ_B , bending stiffness.

highly conserved actin–crosslinking protein (MW = 200 kDa, for dimer) containing an antiparallel homodimer, about ~ 36 nm in size, with actin-binding domains at their amino-terminal [32,33]. α -actinin is localized to lamellipodia as well as the base of filopodia [10,34]. α -actinin can form either tight or loose bundles, entangled isotropic networks, or combinations of the two by crosslinking filaments with variable angles [24,35–37]. Bundles crosslinked by α -actinin have a similar shear stiffness compared to fascin–actin bundles [20] and show elastic response to mechanical deformations [38].

Both fascin- and α-actinin-induced actin bundle formation take place within the cytoplasm crowded with high concentrations of macromolecules. The total concentration of macromolecules within the eukaryotic cells has been estimated to be in the range of ~ 50-400 mg⋅mL⁻¹ [39]. Macromolecular crowding has been shown to affect the polymerization kinetics of actin and nucleotide-dependent actin filament stability [40–45]. Moreover, depletion forces raised by macromolecular crowding can result in the formation of actin bundles [46,47] or networks [48] without crosslinkers. Although many studies have explored the effects of crowding on actin, the way crowding affects interactions between actin-binding proteins (ABPs) and actin filaments is not well understood. Castaneda et al. [49] recently demonstrated that crowding modulates filament bending mechanics and conformational changes, including helical twists of filaments. We hypothesize that these changes in filament mechanics and conformations by crowded environments may also potentially affect fascin or α-actinin binding to filaments and subsequent bundling activities. However, the interplay between the two crosslinking proteins and solution crowding in terms of bundling is unknown.

Here, we investigate how macromolecular crowding modulates the organization and mechanical properties of actin bundles crosslinked by fascin and α -actinin. Utilizing total internal reflection fluorescence (TIRF) and atomic force microscopy (AFM) imaging, we show that macromolecular crowding affects the packing of both fascin- and α -actinin bundles and has a stronger impact on fascin bundle stiffness than on αactinin bundle mechanics. All-atom molecular dynamics (MD) simulations indicate that crowding affects interaction energy and interhydrogen bonds between actin-crosslinking proteins and filaments. The findings suggest a mechanism associated with actin bundle assembly and mechanics controlled by crosslinking proteins in the presence of crowding, which deepens the understanding of cytoskeletal organization in crowded cellular environments.

Materials and methods

Proteins and sample preparations

Actin was purified from rabbit skeletal muscle acetone powder (Pel-Freez Biologicals Inc., Rogers, AR, USA) and gel-filtered over Sephacryl S-300 equilibrated in buffer A (2 mm Tris/HCl, 0.2 mm CaCl₂, 1 mm NaN₃, 0.2 mm ATP, 0.5 mm DTT, pH 8.0) as described in Ref. [49]. Rhodamine rabbit skeletal muscle actin (> 99% purity) was purchased from Cytoskeleton, Inc. (Denver, CO, USA). Ca2+-actin monomers were converted into Mg²⁺-actin monomers by the addition of 0.2 mm EGTA and MgCl2, equal to the initial concentration of G-actin plus 10 µm for 5 min; then, 1/ 10th volume of 10x polymerization buffer (500 mm KCl. 20 mm MgCl₂, 100 mm imidazole, pH 7.0, 10 mm ATP, and 10 mm DTT) was added and incubated at room temperature ($T \sim 22$ °C) for 1 h, as described in Ref. [49]. Bundle formation was induced by adding human recombinant protein fascin with a His-tag (Novus Biologicals, Littleton, CO, USA) or rabbit skeletal muscle α-actinin (Cytoskeleton, Inc.) in the polymerization buffer containing crowding agents: polyethylene glycol (PEG) (MW = 8000 Da) (Fisher, Waltham MA, USA), sucrose (MW = 342 Da) (Sigma, Saint Louis, MO, USA), or Ficoll 70 (MW = 70000 Da) (GE Healthcare, Chicago, IL, USA) at varying concentrations. Crowder concentrations were 1% w/w, 3% w/w, and 5% w/w (~ 10-50 mg·mL⁻¹) for PEG, 10% w/w, 30% w/w, and 50% w/w (~ 100-600 mg·mL⁻¹) for sucrose, and 5% w/w, 10% w/w, and 20% w/w (~ 50-200 mg·mL⁻¹) for Ficoll. The concentrations of crowding agents were chosen to emulate the estimated concentrations of macromolecules within the cytoplasm. In particular, we chose the concentrations for PEG and sucrose based on our recent study [49], which demonstrated the effect of crowding on actin filament mechanics and structure. The concentrations of Ficoll were selected following a previous study [41] that showed how macromolecular crowding affects actin polymerization kinetics. We chose the concentrations of crowders 'below' a threshold concentration that would start forming bundles (PEG < 5% w/w [46], sucrose < 50% w/w, and Ficoll < 20% w/w (Fig. S1)), in order to separate effects of crosslinking proteins from depletion-induced bundling.

Low-speed cosedimentation assay

To evaluate the bundling activity of actin–crosslinking proteins, a low-speed co-sedimentation assay was performed using a modified protocol as previously described in Ref. [25]. Actin monomers were polymerized into filaments for 1 h at room temperature before being equilibrated in the presence of crowders for 1 h. As control samples, 5 μm of F-actin alone, 2.5 μm fascin alone, and 1 μm α-actinin alone were incubated in dilute polymerization buffer or crowded

buffers containing PEG (1%, 3%, or 5% w/w), sucrose (10%, 30%, or 50% w/w), or Ficoll 70 (5%, 10%, or 20% w/w) for 1 h at room temperature. For co-sedimentation assays, 5 µm of F-actin was incubated with 2.5 µm fascin or 1 μM α-actinin for 1 h at room temperature in the presence of PEG (1%, 3%, or 5% w/w), sucrose (10%, 30%, or 50% w/w), or Ficoll 70 (5%, 10%, or 20% w/w). The molar ratios of actin to fascin or α-actinin used for these sedimentation assays were chosen for effective actin bundle formation as shown in previous studies [31,50]. Crosslinking protein-induced bundles were spun at 8644 g for 1 h at 4 °C using a Sorvall MTX 150 (Thermo Fisher Scientific, Waltham, MA, USA). Due to the high viscosity of solution containing crowding agents, the top 20% supernatant and bottom 20% pellets were collected, transferred to separate tubes, and resuspended with polymerization buffer. The supernatants and pellets for each condition were separated by SDS/PAGE using 12% resolving gel at 80 V for 2 h. The gels were stained by Coomassie blue staining and imaged with ChemiDoc (Bio-Rad, Hercules, CA, USA). The relative amounts of protein bands were analyzed by IM-AGE LAB software (Bio-Rad) as described in Ref. [51].

TIRF microscopy imaging and mechanics data analysis

Actin bundles (50% rhodamine-labeled, 1 μM) induced by fascin or α-actinin (0.5 μм) were equilibrated for 1 h in the presence of crowding agents at room temperature prior to TIRF imaging. Bundle samples were diluted in optical imaging buffer (10 mm imidazole pH 7.0, 50 mm KCl, 2 mm MgCl₂, 1 mm ATP, 1 mm DTT, 0.15 m glucose, 1 mg·mL⁻¹ catalase, and 0.1 mg·mL⁻¹ glucose oxidase) [49,52]. Actincrosslinking protein-induced bundles were immobilized on coverslips coated with 0.01% v/v poly-L-lysine (Sigma-Aldrich, St. Louis, MO, USA) which produces a weak electrostatic force to adhere biopolymers to glass surfaces while maintaining the fluctuation of bundle as the previous studies used [52]. Bundle images were acquired at room temperature using a Nikon Eclipse Ti TIRF microscope equipped with a Hamamatsu ImagEM X2 CCD camera, 100X oil immersion objective (numerical aperture 1.49), and Nikon LU-N4 laser (Nikon Instruments Inc., Melville, NY, USA). NIKON IMAG-ING SOFTWARE (NIS)-ELEMENTS (ver. 5.02) was used to capture images (pixel size = $0.16 \mu \text{m} \cdot \text{pixel}^{-1}$) (Nikon Instruments Inc., Melville, NY, USA).

The number of filaments per each bundle was estimated from the sum of fluorescence intensities across the bundle divided by that of one filament using NIS-ELEMENTS Advanced Research software (ver. 5.02) [52,53]. Actin bundle length (L) and bending persistence length ($L_{\rm p}$) were analyzed using IMAGEI, Persistence [54], and ORIGINLAB 8.5 (OriginLab Corp, Northampton, MA, USA). Bundle $L_{\rm p}$ was calculated from the two-dimensional average cosine correlation (<C(s)>) of the tangent angle (θ) along the

segment length (s) of a bundle by fitting to Eqn (1) (where A is a scaling factor) as described in Ref. [52,54].

$$\langle C(s) \rangle = \langle cos[\theta(s) - \theta(0)] \rangle = A \cdot e^{-x/2L_p}.$$
 (1)

The flexural rigidity of the bundle (κ_B) was calculated following Eqn (2), in which L_p is the persistence length and k_BT is the thermal energy [52,54].

$$\kappa_{\rm B} = L_{\rm p} k_{\rm B} T. \tag{2}$$

The longitudinal Young modulus of fascin bundles ($E_{\rm B}$) was estimated following Eqn (3), where I denotes the second moment of inertia of bundles, respectively [55,56].

$$E_{\rm B} = \frac{\kappa_{\rm B}}{I} = \frac{L_{\rm p} k_{\rm B} T}{I}.$$
 (3)

The second moment of inertia (*I*) was calculated following Eqn (4) with the assumption that fascin-induced bundles are rod-like structures [57] with radius (*r*) measured from AFM images shown below.

$$I = \frac{\pi r^4}{4}. (4)$$

Atomic force microscopy imaging

Mica substrates were freshly cleaved and coated with 30 μL of 0.1% v/v (3-aminopropyl) triethoxysilane (APTES) for 10 min to obtain a positively charged surface and improve adherence of fascin- or α-actinin-induced bundles [58,59]. The APTES-coated mica substrates were then rinsed with deionized water and dried with a gentle stream of compressed air [58,59]. Five microlitre of fascin- or α-actinin-induced actin bundles ([actin] = 5 μM, molar ratio of actin to fascin or α-actinin 2:1 or 5:1) was deposited onto the APTES-coated mica and allowed to bind for 3 min [59]. The substrate was rinsed gently with compressed air and dried.

To observe the morphology of actin bundles, height and amplitude images were collected using a Nanoscope IIIA MultiMode AFM System (Bruker, Santa Barbara, CA, USA). Imaging was conducted in ambient conditions and performed in tapping mode using aluminum-coated silicon AFM cantilever tips with a nominal spring constant of ~ 2.7 N·m⁻¹ and nominal resonant frequency of ~ 60–100 kHz (HQ:XSC11/Al BS; Mikromasch, Wilsonville, OR, USA). All images consisted of 512 points × 512 points. Scan sizes varied from 0.5 to 10 μm. Height, length, and FWHM of bundles were quantified by Gwyddion [60].

Statistical analysis

Statistical significance of the numbers of filaments per bundle, bundle persistence lengths, and bundle diameters was determined using ORIGINLAB 8.5 softwareby conducting

multiple analysis of variance (ANOVA) with *post hoc* Tukey's test. Notation for probability (P-value): n.s., not significant (P > 0.05); *, P < 0.05; **, P < 0.01; ***, P < 0.001.

Molecular modeling for actin/cross-linking protein complex in the presence of crowders

To investigate the effects of crowding on the interactions between F-actin and crosslinking proteins, we employed the molecular system of an F-actin using a recent filament model revealed by high-resolution cryo-electron microscopy (cryo-EM) (PDB ID: 3J8I) [61]. The filament was constructed using four actin subunits [62]. For actin-crosslinking proteins, we used full-length fascin (PDB ID: 3P53) [25] and the calponin homology (CH) 1 domain of α -actinin, adapted from a filament decorated with CH1 domain of αactinin (residues from 26 to 146) (PDB ID: 3LUE) [63]. Fascin was bound to the filament using Z-dock web server [64] based on the known binding sites of fascin to F-actin [25,65]. Subsequently, we selected the lowest potential energy upon 10 000 times of energy minimization among the outcomes of Z-dock molecular docking simulation. To bind the CH1 domain of α-actinin to F-actin, we followed the structural composition of actin/α-actinin complex from the Galkin model [66]. Then, to evaluate the interaction of fascin or CH1 domain of α-actinin near the binding interface, we set an initial distance of 15 Å between the filament and each crosslinking protein.

Three crowders including PEG ($M_W = 385.25 \text{ g} \cdot \text{mol}^{-1}$), sucrose ($M_W = 389.52 \text{ g} \cdot \text{mol}^{-1}$), and Ficoll 400 ($M_W =$ 432.8 g·mol⁻¹) were considered. Of note, Ficoll 400 was chosen for molecular modeling because the structure of Ficoll 70 is not available. We performed 1000 times of energy minimization and 10 ns of equilibration simulations for each crowder. Subsequently, we solvated PEG (n = 20), sucrose (n = 40), and Ficoll (n = 20) near the filament-crosslinking protein complex with a minimal distance of 5 Å using PACKMOL [67]. In the case of sucrose, the number of molecules was twice as much as PEG or Ficoll in order to produce similar crowding concentrations considering its smaller size compared to the other two polymeric crowders. The simulated crowding concentrations were chosen to mimic the highest concentration of experimental crowding conditions when considering the size of crowders. The concentration of crowders in the simulation (C) is converted as follows; C_{PEG, with fascin} ~3.6 mm, ~6.17 mm, $C_{\text{Ficoll, with fascin}}$ ~3.11 mm, $C_{\text{sucrose, with fascin}}$ ~5 mm, $C_{\text{sucrose, with }\alpha\text{-actinin}}$ ~7.5 mм, $C_{\text{PEG, with }\alpha\text{-actinin}}$ ~3.39 mm. The explicit models of C_{Ficoll, with α-actinin} filament-crosslinking protein complexes with molecular crowders were built using the TIP3P water model with a conditional 15 Å of water padding. To neutralize the system and mimic experimental conditions, 2 mm MgCl₂ was solvated near the complexes.

Molecular dynamics simulations and analysis of interactions between filament and crosslinking proteins

After energy minimization, we performed 20-ns equilibrium MD simulations on each actin bundle complex in the absence or presence of crowders using NAMD 2.12 package [68]. CHARMM27 force field (FF) with CMAP corrections for proteins, CHARMM35 ether FF for PEG [69], CHARMM CGenFF for Ficoll 400 [70], and CHARMM36 carboxyl FF for sucrose were used [71]. Equilibrium MD simulations were carried out with consideration of the NPT ensemble (constant number of atoms, P = 1 bar and T = 300 K) and time step of 2 fs. Upon completion of the MD simulations, we analyzed the radius of gyration (R_g) and root-mean-square deviation (RMSD) of crosslinking proteins as well as F-actin with crosslinking proteins using visual molecular dynamics (VMD) [72]. To assess the degree of binding interactions and characteristics near the filament and unbound crosslinking protein interface, we calculated the inter-hydrogen bond and interaction energy. The number of inter-hydrogen bonds between filament and crosslinking proteins was obtained using the hydrogen plugin of VMD with a distance inferior to 3.5 Å and angle superior to 120° [72]. Using the same approach, interaction energy was calculated using the NAMD energy plugin of VMD 1.9.1.

Results and Discussion

Macromolecular crowding modulates fascininduced bundle organization and mechanics

We first evaluated how crowding affects the bundling activities of fascin using a low-speed co-sedimentation assay (at the average centrifugation speed of 8,644 g) [25,31]. As an assay control, F-actin alone ([actin] = 5 μm) in the absence or presence of crowding agents (PEG, sucrose, and Ficoll) was assessed (Fig. S1). The amount of F-actin in the supernatant significantly increased in sucrose and Ficoll (% F-actin is > 80%) (Fig. S1a,b). In the presence of PEG, the amount of actin in the supernatant showed a slight decrease compared to the control of up to 17%. Filament formation for F-actin control with crowders was confirmed by TIRF microscopy imaging (Fig. S1c). Next, low-speed co-sedimentation assays were performed after prepolymerized F-actin was incubated with fascin at a 2:1 (actin to fascin) molar ratio. Most of the F-actin was found in the pellet and around 50-60% fascin was cosedimented with F-actin, confirming fascin formed actin bundles (Fig. S2). We observed a slight decrease in the percent of fascin as well as actin in the pellet at 50% w/w sucrose (Fig. S2c).

To investigate how crowding affected bundle organization and mechanical properties, we directly visualized fascin-induced bundles (50% rhodamine-labeled, molar ratio of actin to fascin = 2:1) in the presence of varying concentrations of crowders by TIRF microscopy (Fig. 1 A). We analyzed the cross-sectional fluorescence intensities of bundles to estimate the number of filaments per bundle [52,53,73]. Overall, the number of filaments per bundle increased with a rise in crowder concentrations by approximately 1.7-fold at the highest concentration of crowder (Fig. 1B). The average bundle length (L) did not change significantly in the presence of crowding agents $[L_{\rm control} = 2.55 \pm 1.32 \, \mu \text{m} \, (\text{mean} \pm \text{SD}), L_{\rm PEG,5\% \, w/w} =$ $L_{\text{sucrose, }50\% \text{ w/w}} = 2.77 \pm 1.41 \text{ }\mu\text{m},$ $2.33 \pm 1.14 \, \mu m$ $L_{\text{Ficoll } 20\% \text{ w/w}} = 2.68 \pm 1.43 \text{ }\mu\text{m}$].

We also compared the bending persistence length (L_p) of fascin-induced bundles, with or without crowding agents, obtained from the two-dimensional cosine correlation [52,54] (Fig. 1C). For our experiments, glass slides were passivated by poly-L-lysine allowing for weak electrostatic interactions to enable visualization and mechanical analysis of bundles [74]. Of note, the thermal fluctuation of bundles [31] was performed and no observable difference was quantified between the methods of analysis ($\pm 10\%$). Fascin induced stiff bundles $(L_p = 46.81 \pm 3.71 \,\mu\text{m})$ at the 2:1 molar ratio of actin to fascin in the absence of crowders. This value is much lower than the reported value (L_p up to 166 μm) at the same molar ratio analyzed from the path of bundles propelled by surface-adhered myosin in a previous study [31]. This discrepancy may be attributed to thicker bundles observed in the study [31] with higher number of filaments per bundle $(n = 18 \pm 4)$, compared to our estimation for fascincrosslinked bundles $(n = 6.0 \pm 2.2)$. Meanwhile, average bending L_p significantly reduced with PEG concentrations of 3% and 5%, $L_{p \text{ PEG, 3% w/w}} =$ $29.62 \pm 5.31 \mu m$ corresponding to a 37% reduction, and $L_{\rm p, PEG, 5\%, w/w} = 25.32 \pm 1.12 \,\mu \text{m}$ corresponding to a 46% reduction with respect to the control (Fig. 1C). Sucrose did not induce stiffer bundles compared to the control (Fig. 1C). In the case of Ficoll, the average bending L_p of fascin bundles peaked at 10% w/w ($L_{p \text{ Ficoll}, 10\%}$ $w/w = 95.94 \pm 12.96 \mu m$) (Fig. 1C). Using L_p values, we estimated the bending stiffness (κ_B) of fascin bundles at room temperature. κ_B varied in the presence of crowding agents compared to control ($\kappa_{B, \, control} = 2.0 \times$ $10^{-25} \text{ N} \cdot \text{m}^2$), with values of $\kappa_{B, PEG} = 1.0 -1.9 \times$ $10^{-25} \text{ N} \cdot \text{m}^2$, $\kappa_{\text{B. sucrose}} = 1.5 - 2.0 \times 10^{-25} \text{ N} \cdot \text{m}^2$, and $\kappa_{\rm B,\ Ficoll} = 2.3 - 3.9 \times 10^{-25}\ {\rm N\cdot m^2}$. These changes are similar to those observed in the case of divalent cation-induced bundles [52], although the bundles are less rigid than comparable crosslinking protein-induced bundles

reported in Ref. [20], representing $\kappa_{B, \text{ control}} = 2.0 \times 10^{-24} \text{ N} \cdot \text{m}^2$.

PEG and Ficoll showed different effects on mechanics of fascin-induced bundles. PEG 8000 (MW = 8 kDa) is a linear polymeric crowder with a hydrodynamic radius of ~ 24.5 Å [75], whereas Ficoll 70 (MW = 70 kDa) is a highly branched polymer with a hydrodynamic radius of ~ 40 Å [75]. Recent studies have described how crowder structure affects DNA packing and dynamics [76] as well as persistence length of other worm-like chain polymers [77]. Furthermore, changes in the fascin-induced bundle packing and stiffness can be attributed to the different sizes and conformations of crowding agents. For example, in a recently resolved high-resolution structure, Jansen et al. [25] showed how a PEG molecule tightly binds to the cleft formed between the two actin-binding sites of fascin. This suggests that crowders present near fascin or filaments can reduce their binding interactions.

Macromolecular crowding influences the organization of α -actinin-induced bundle/ networks, while weakly affecting α -actinin bundle mechanics

Bundling activities of α -actinin were evaluated using low-speed co-sedimentation assay in the same way as fascin bundles described above (Fig. S3). Prepolymerized F-actin was incubated with α -actinin at a molar ratio of 5:1 (actin to α -actinin) without or with crowders and centrifuged at 8644 g. The amount of α -actinin and actin in the pellet slightly increased with increasing PEG and Ficoll concentrations, except 20% w/w Ficoll (Fig. S3c,d). However, increasing concentrations of sucrose drastically reduced the amount of α -actinin and actin in the pellet, indicating the bundling activity of α -actinin was decreased in the presence of sucrose.

TIRF images showed crowding altered the morphology of α -actinin-induced bundles/networks, depending on the specific crowding agent (Fig. 2). Overall, polymeric crowders (PEG and Ficoll) induced well-defined bundles, whereas the monomeric crowder (sucrose) instead formed mesh-like networks (Fig. 2A). Depending on the molar ratio of α -actinin to F-actin, α -actinin has been shown to form either bundles or networks [36,37,78]. Here, when maintaining the same molar ratio of actin to α -actinin, α -actinin induced either bundles or mixtures of bundles/networks depending on the type of crowders (Fig. 2). The different bundle/network formations of α -actinin might be explained through the binding behavior of α -actinin [24]. α -actinin can crosslink two single actin

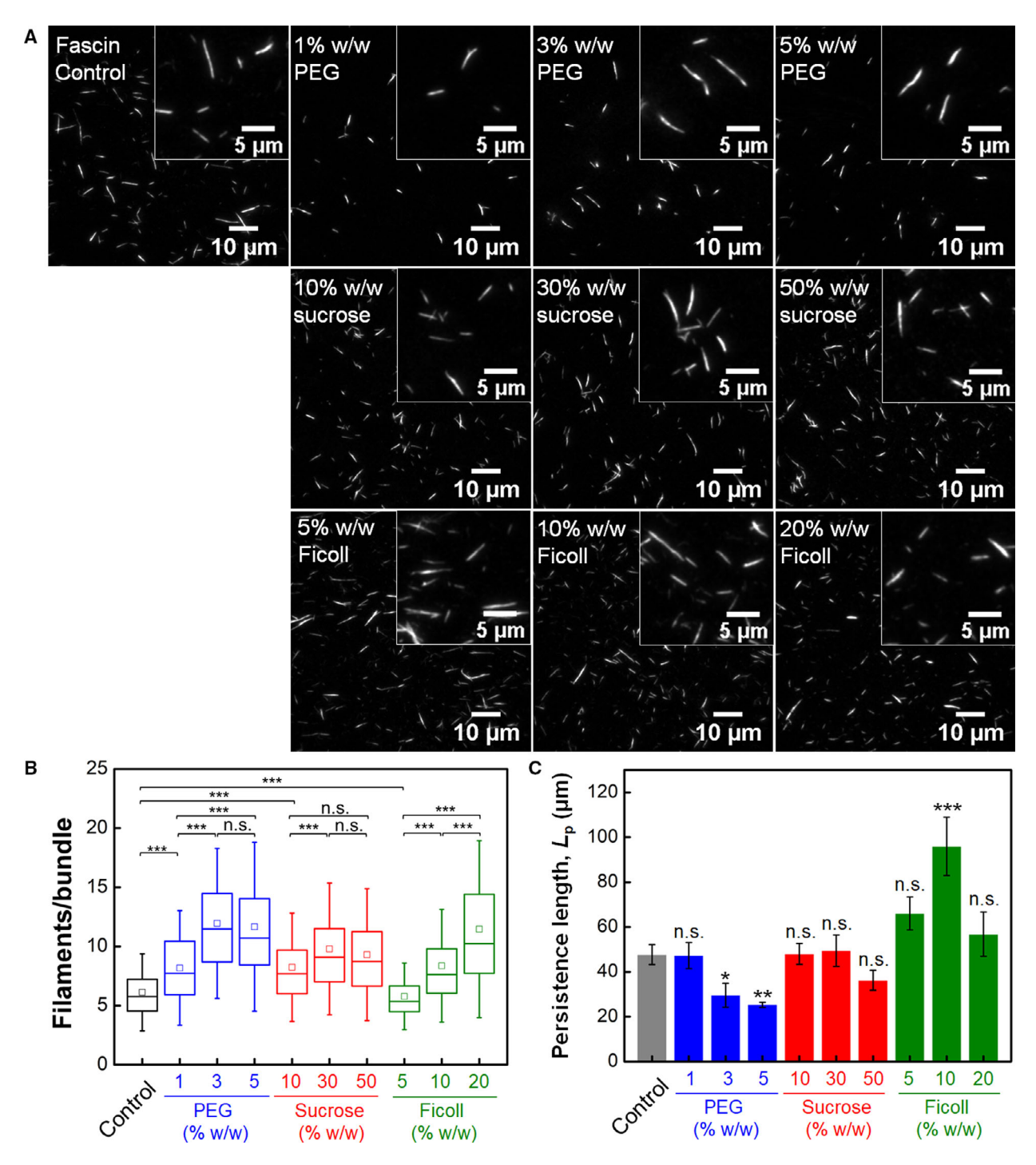


Fig. 1. Effects of crowding on fascin-induced bundles. (A) Representative TIRF microscopy images of fascin-induced bundles (the molar ratio of actin to fascin = 2:1). 1 μM of actin filaments (50% rhodamine-labeled) and 0.5 μM of fascin were incubated in dilute polymerization buffer (10 mM imidazole, pH 7.0, 50 mM KCl, 2 mM MgCl₂, 1 mM ATP, and 1 mM DTT) or buffers containing crowding agents (1–5%w/w PEG, 10–50% w/w sucrose, or 5–20% w/w Ficoll) for 1 h at room temperature prior to imaging (scale bar, 10 μm). The insets are zoom-ins of each TIRF image (scale bar, 5 μm). (B) The number of filaments per bundle analyzed from cross-sectional fluorescence intensities without or with crowders. The box represents the 25–75% of data, whiskers indicate standard deviation (SD), and the middle square is the mean. (C) Bending persistence length (L_p) of fascin bundles without or with crowders. Sample size: $N_{control} = 291$, $N_{1\%w/w}$ PEG = 222, $N_{3\%w/w}$ PEG = 241, $N_{5\%w/w}$ PEG = 240, $N_{10\%w/w}$ sucrose = 323, $N_{30\%w/w}$ sucrose = 299, $N_{50\%w/w}$ sucrose = 357, $N_{5\%w/w}$ Ficoll = 389, $N_{10\%w/w}$ Ficoll = 414, $N_{20\%w/w}$ Ficoll = 502. P values were determined with one-way ANOVA and P00 Tukey's test. (n.s., not significant; *P0.05; *P0.01; ***P0.001).

filaments when they are positioned within a wide range of angles between them $(16-165^{\circ})$ [24]. In addition, α -actinin network/bundle formation is highly affected by the mobility of actin filaments [50]; therefore, it is possible that filament stiffening and overtwisting caused by crowding [49] may affect the binding of α-actinin. Falzone et al. [50] revealed that the bundling assembly rate of α-actinin-induced bundle is highly affected by solution viscosity. As the viscoelasticity of microenvironment became from viscous to viscoelastic fluid, highly mobile actin filaments form bundles faster, but as the microenvironment reaches to the elastic solid, the bundle formation rate decreased [50]. A highly elastic microenvironment due to crowding reduces filament mobility and affects the length of filament where it does not overcome the threshold distance between F-actins to form α-actinin-induced bundle, thereby impeding crosslink-mediated bundle formation.

The number of filaments per α -actinin-induced bundle decreased with increasing concentrations of crowding agents (Fig. 2B). PEG induced well-defined α-actininactin bundles, where bundle length (L) decreased increasing **PEG** concentrations with $(L_{\rm control} =$ $L_{\rm PEG, 1\% \ w/w} = 8.49 \pm 5.27 \ \mu {\rm m},$ $8.41 \pm 3.53 \, \mu m$ $L_{\rm PEG, 3\% \ w/w} = 4.14 \pm 2.80 \ \mu \text{m}$, and $L_{\rm PEG, 5\% \ w/w} =$ $3.09 \pm 1.91 \mu m$). We noted that α -actinin induced longer bundles in the presence of Ficoll ($L_{\rm control} = 8.41 \pm$ 3.53 μ m, $L_{\text{Ficoll.}}$ 5% $_{\text{W/W}}$ = 12.10 \pm 6.50 μ m, $L_{\text{Ficoll.}}$ 10% $_{\text{W/W}}$ = $11.15 \pm 6.89 \, \mu m$ $L_{\text{Ficoll, 20\% w/w}} = 12.01 \pm 6.67 \,\mu\text{m}$). Sucrose induced shorter α -actinin bundles within mesh-like networks in a concentration-dependent manner ($L_{\text{control}} =$ $8.41 \pm 3.53 \, \mu m$ $L_{\text{Sucrose, }10\%\text{w/w}} = 8.89 \pm 0.88 \text{ } \mu\text{m},$ $L_{\text{Sucrose, }30\% \text{ w/w}} = 2.96 \pm 0.31 \text{ }\mu\text{m}$). At 50% w/w sucrose, α-actinin did not induce bundles, but rather formed meshlike networks. Only few bundles with short lengths were observed; however, they were all embedded in the meshlike networks, as shown in the representative TIRF image (Fig. 2A). For this reason, the number of filaments per bundle and persistence length could not be analyzed. In contrast to fascin bundles, crowding weakly influenced the bending L_p of α -actinin-induced bundles, resulting in rather flexible bundles across all conditions $(L_{\rm p, average} = 9.48 \ \mu {\rm m})$ (Fig. 2C). The average bending stiffness (κ_B) of α -actinin-induced bundle was 4.55 \times $10^{-26} \text{ N} \cdot \text{m}^2$ for control, $2.70-5.30 \times 10^{-26} \text{ N} \cdot \text{m}^2$ for PEG, $2.20-3.97 \times 10^{-26} \text{ N} \cdot \text{m}^2$ for sucrose, and $3.56-4.52 \times$ $10^{-26} \text{ N} \cdot \text{m}^2$ for Ficoll.

Macromolecular crowding modulates the structure of crosslinked actin bundles

To further analyze how crowding affected the structure of fascin- and α -actinin-induced actin bundles at the

molecular scale, we conducted AFM imaging of cross-linked bundles in the absence and presence of crowders (Fig. 3A). In the case of sucrose, the lowest concentration (10% w/w) was selected due to a high density of bundles being attached to the APTES-coated surface, which made it difficult to characterize individual bundles at higher concentrations.

Our results demonstrate that macromolecular crowding reduces the thickness of both fascin and α-actinin-induced bundles (Fig. 3A). The diameter of bundles was calculated from FWHM. As shown in Fig. 3B, the average diameter (D) of control fascin bundles was 230.04 ± 39.19 nm but decreased in the presence of $(D_{\rm fascin, PEG} = 108.21 \pm 32.14 \text{ nm},$ crowding agents $D_{\rm fascin, sucrose} = 123.85 \pm 31.15 \text{ nm},$ $D_{\text{fascin, Ficoll}} =$ 173.47 ± 27.18 nm) (Fig. 3B). The diameter distribution of fascin bundles demonstrated macromolecular crowding reduces bundle dimensions (Fig. S4a). Considering the number of filaments per fascin bundle increased with crowding (Fig. 1B), it can be concluded that fascin forms densely packed bundles in crowded environments. The morphology of α -actinin bundles revealed by AFM exhibited distinct organization, consistent with TIRF results (Fig. 2). α-actinin within the bundle (white dots on bundle) are distinguishable throughout all samples (Fig. 3A), appearing as globular foci, similar to Ref. [79]. The average diameter of control α -actinin bundle was 264.66 \pm 53.3 nm, which is then shown to decrease in the presence of crowding $(D_{\alpha\text{-actinin, PEG}} = 130.24 \pm 37.62 \text{ nm}, \quad D_{\alpha\text{-actinin, Ficoll}} =$ 97.36 ± 36.44 nm). Sucrose reduced the diameter of α -actinin bundles (D_{α -actinin, sucrose} = 52.20 ± 18.15 nm) the most (Fig. S4b). A previous report [80] has shown the processes that are present during initial nucleation phase can affect the distribution of bundle thicknesses, along with the distribution of steady-state thickness for fascin-actin bundles, which can be best-fit by exponential function with a distinct peak. The changes in bundle diameter distribution observed here occurring in the presence of crowding suggest the possibility of an altered nucleation due to crowding.

The longitudinal Young modulus of fascin bundles $(E_{\rm B})$ can be estimated based on bending stiffness $(\kappa_{\rm B})$ calculated from $L_{\rm p}$ (Fig. 1) and bundle diameters measured by AFM [56] (Fig. 3). The Young modulus depends not only on $\kappa_{\rm B}$ but also on bundle geometry [57], which can be assumed to be a rod-like structure for fascin bundles [80]. Interestingly, the longitudinal $E_{\rm B}$ of fascin–actin bundles increased by 12-fold in the presence of PEG and sucrose, and threefold with Ficoll $(E_{\rm B,\;control}=1.22\pm0.37\;{\rm kPa},\;E_{\rm B,\;PEG}=14.79\pm2.29\;{\rm kPa},\;E_{\rm B,\;sucrose}=14.38\pm2.81\;{\rm kPa},\;E_{\rm B,\;Ficoll}=4.14\pm1.39\;{\rm kPa})$ (Fig. S5). Both TIRF and AFM

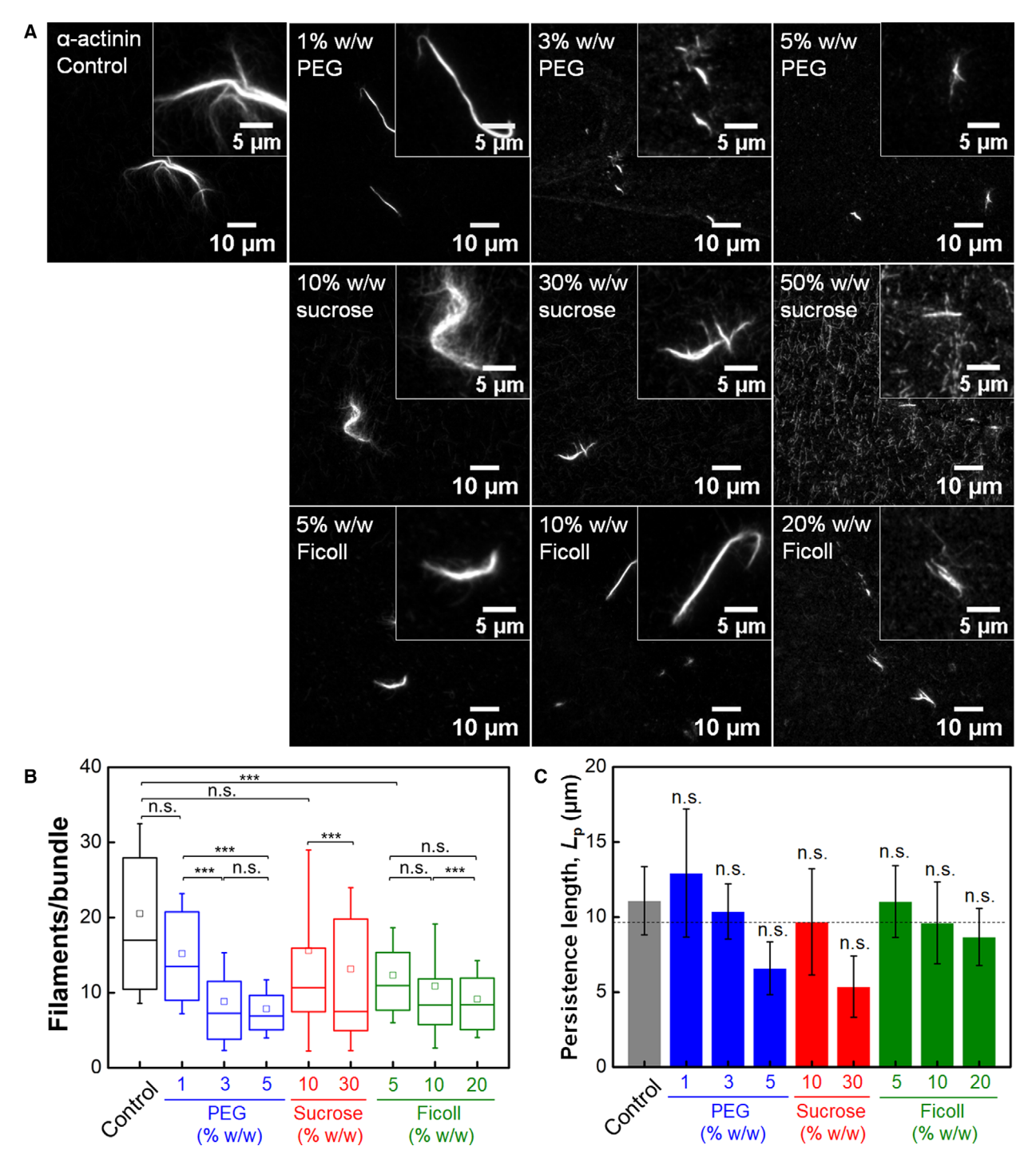


Fig. 2. Effects of crowding on α-actinin-induced bundles. (A) Representative TIRF microscopy images of α-actinin-induced bundles (the molar ratio of actin to α-actinin = 2:1). 1 μM of actin filaments (50% rhodamine-labeled) and 0.5 μM of α-actinin were incubated in dilute polymerization buffer (10 mM imidazole, pH 7.0, 50 mM KCl, 2 mM MgCl₂, 1 mM ATP, and 1 mM DTT) or buffers containing crowding agents (1–5%w/w PEG, 10–50% w/w sucrose, or 5–20% w/w Ficoll) for 1 h at room temperature prior to imaging (scale bars, 10 μm). The insets are zoom-ins of each TIRF image (scale bar, 5 μm). (B) The number of filaments per bundle without and with crowders. The box represents the 25–75% of data, whiskers indicate SD, and the middle square is the mean. (C) Bending persistence length (L_p) of α-actinin-crosslinked bundles without and with crowders. The dashed line represents the average L_p (9.47 μm) of all the analyzed bundles. Sample size: $N_{\text{control}} = 84$, $N_{1\%\text{w/W}\text{ PEG}} = 155$, $N_{3\%\text{w/W}\text{ PEG}} = 143$, $N_{5\%\text{w/W}\text{ PEG}} = 126$, $N_{10\%\text{w/W}\text{ sucrose}} = 146$, $N_{30\%\text{w/W}\text{ sucrose}} = 97$, $N_{50\%\text{w/W}\text{ sucrose}} = 28$, $N_{5\%\text{w/W}\text{ Ficoll}} = 152$, $N_{10\%\text{w/W}\text{ Ficoll}} = 100$, $N_{20\%\text{w/W}\text{ Ficoll}} = 121$. p values were determined with one-way ANOVA and $post\ hoc\ Tukey$'s test (n.s., not significant; *P < 0.05; **P < 0.01; ***P < 0.001).

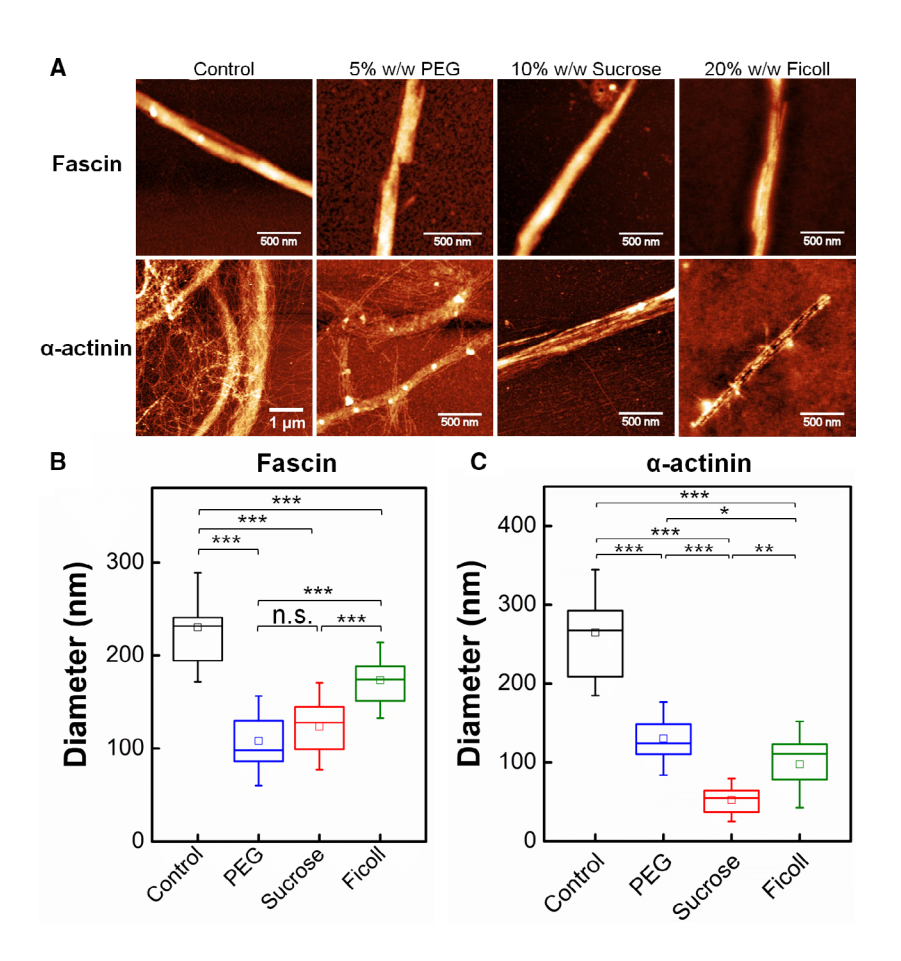


Fig. 3. The structure of fascin- and α-actinin-induced bundles in crowded environments. (A) AFM height images of fascin- and α -actinin-induced bundles with various crowding conditions. The molar ratio of unlabeled actin to crosslinking proteins was 2:1 except for control of α-actinin-induced bundle (5:1) ([actin] = 5 μ M). Actin filaments were incubated with fascin or α-actinin in dilute polymerization buffer (10 mm imidazole. pH 7.0, 50 mм KCl, 2 mм MgCl₂, 1 mм ATP, and 1 mm DTT) or buffers containing crowding agents (5% w/w PEG, 10% w/w sucrose, or 20% w/w Ficoll) for 1 h at room temperature prior to imaging. All scales bars = 500 nm except α -actinin control scale bar = 1 μ m. Diameters of (B) fascin-induced actin bundles and (C) αactinin-induced bundles under varying crowding conditions. Bundle diameters were determined by the full width at half maximum (FWHM) on the AFM images. The box represents the 25-75% of data, whiskers indicate SD, and the middle square is the mean. P values were determined with one-way ANOVA and post hoc Tukey's test (n.s., not significant; **P* < 0.05; ***P* < 0.01; ****P* < 0.001).

images of the α -actinin-crosslinked bundles showed that bundles were heterogeneous in thickness, in particular for the control sample, which was evident from bundle thickness distribution (Fig. S4b). Given this nonuniform thickness, the assumption of rod-like structure would not be appropriate to estimate the $E_{\rm B}$ of α -actinin-crosslinked bundles.

Macromolecular crowding reduces binding interactions between crosslinking proteins and filaments

To evaluate binding interactions between actin filaments and fascin or α -actinin in crowded environments, we performed equilibrium all-atom MD simulations (Fig. 4). In the case of α -actinin, the CH1 domain (residues from 26 to 146) that contains main actin-binding sites [62] was used for the simulations. We first analyzed the $R_{\rm g}$ and RMSD of crosslinking proteins (fascin or CH1 domain of α -actinin) and F-actin–crosslinking protein complexes in order to evaluate their conformational changes associated with crowding. The overall $R_{\rm g}$ and

RMSD of both crosslinkers and F-actin-crosslinking protein complexes in the presence of crowders were similar to control (Figs S6 and S7), supporting that crowding did not significantly affect the conformations of crosslinking proteins, nor those of F-actin-crosslinker complexes.

To determine the bundling interactions, we analyzed the interaction energy, which is the combined electrostatic energy and van der Waals (vdW) energy, between the actin and actin bundling protein complex. During the 20-ns MD simulations, crowding increased the interaction energy between filament and fascin or CH1 domain of α-actinin (Fig. S8). Furthermore, the average interaction energy during the last 10 ns increased and became less negative with sucrose and Ficoll. In the presence of PEG, the interaction energy values were similar to the control sample (Fig. 5A, Table 1). In addition, crowding decreased the overall number of hydrogen bonds at the binding interface between filaments and fascin or CH1 domain of α-actinin (Fig. 5B, Table 2). Both interaction energy and hydrogen bonding analysis indicated that crowders

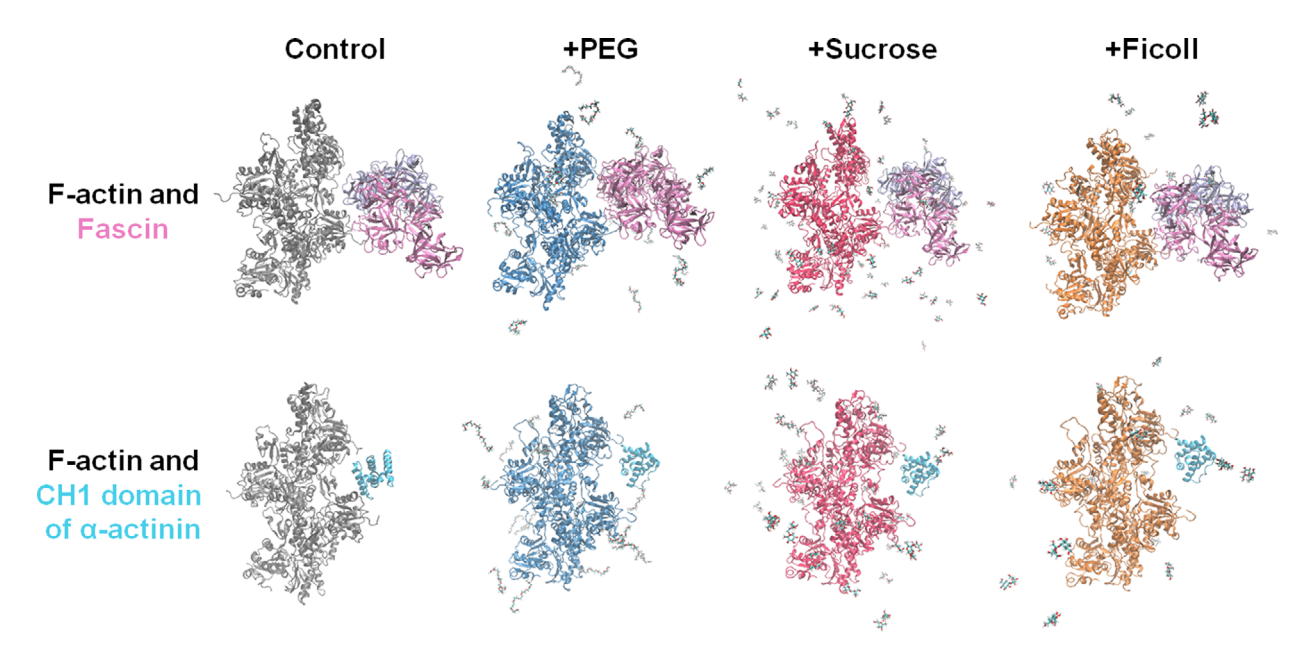


Fig. 4. Conformations of actin filament (F-actin) with fascin or CH1 domain of α-actinin without or with crowders.

destabilized the interaction between F-actin and fascin or CH1 domain of α -actinin. Changes in bundle packing and crosslinked actin bundle mechanics discussed above may be related to this reduced binding raised by macromolecular crowding.

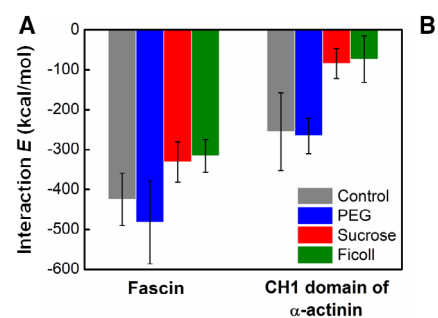
Proposed mechanism and future outlook

Our experimental and computational results enable the formulation of a mechanism for fascin and α -actinin-induced bundle formation under crowded conditions (Fig. 6). Altered stiffness and helical twist of filaments in the presence of crowding [49] potentially modulate binding interactions offascin and α -actinin, resulting in different organizations and mechanics of crosslinked bundles. In the case of fascin, solution crowding results in densely packed bundles and disrupts binding of fascin to actin filaments (Fig. 6A) based on the increased interaction energy and

decreased number of hydrogen bonds between fascin and F-actin (Fig. 5A,B). In the case of α-actinin (Fig. 6B), polymeric crowders induce shorter, thinner, and disconnected bundles, whereas monomeric crowders induce embedded bundles in networks rather than individual bundles, while circumventing significant changes in mechanics. The size of crosslinkers (fascin: ~ 5 nm; α-actinin: ~ 35 nm) may affect interfilament distance leading to the energetic cost for bending [20]. In addition, crowders influence the binding behavior of fascin and α-actinin within bundles, potentially leading to different mechanical propcrosslinked erties of bundles. Viscoelasticity, depending on the crowding solution concentration, may also affect the α-actinin-induced bundle formation by modulating the bundling assembly rate of α -actinin-induced bundle [50].

Crowding may cause various effects in the interactions between actin and crosslinking proteins

Fig. 5. Interaction energy and interhydrogen bond analysis. (A) Average interaction energy (\pm SD) and (B) the number of hydrogen bonds (\pm SD) between filaments and fascin or CH1 domain of α -actinin in the absence or presence of crowders, for the last 10 ns of the 20-ns equilibrium all-atom molecular dynamics (MD) simulations.



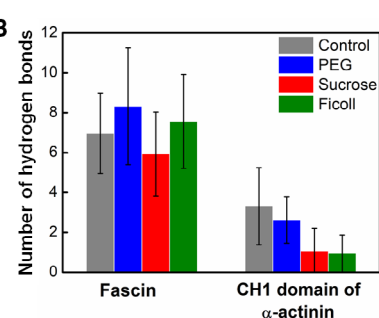


Table 1. The average interaction energy (\pm SD) between actin filament and fascin or CH1 domain of α -actinin in the absence or presence of crowders for the last 10 ns of the 20-ns MD simulations.

Crowder	Fascin (kcal·mol ⁻¹)	CH1 domain of α-actinin (kcal·mol ⁻¹)
Control (no crowder) PEG Sucrose	-424.51 (±65.65) -482.19 (±103.69) -330.83 (±50.99)	-254.66 (±97.28) -265.61 (±44.70) -83.99 (±37.41)
FicoII	-315.29 (±40.94)	-72.85 (±58.63)

Table 2. The average number of hydrogen bonds (\pm SD) formed between actin filament and fascin or CH1 domain of α -actinin without or with crowders for the last 10 ns of the 20-ns MD simulations.

Crowder	Fascin	CH1 domain of α-actinin
Control (no crowder)	6.96 (±2.01) 8.32 (±2.92)	3.31 (±1.93) 2.63 (±1.17)
Sucrose	5.93 (±2.11)	1.06 (±1.16)
FicoII	7.57 (\pm 2.36)	0.95 (±0.92)

depending on the distinct structures of crowders. The extent of packing configurations is different with a linear polymeric crowder such as PEG or with a branched polymeric crowder such as Ficoll [76]. Of note, sucrose induces less osmotic pressure than Ficoll [81]. The differing hydrodynamic dimensions of crowding agents may affect the formation of bundles. For example, Gagarskaia et al. [82] showed PEG 8k of hydrodynamic radius (24.5 Å) [75] is similar to globular actin and has a greater stabilization effect on the actin structure than Dextran 70k. Furthermore, a recent study supported a theoretical prediction that the crowding effects can be dependent on the shape of proteins [83]. This is in line with our observations given that fascin functions as a monomer while α -actinin associates in dimers.

Excluded volume effects raised by crowding have been shown to lead to microviscosity, which can affect the rates of actin polymerization as well as protein diffusion [42,43,84]. Consequently, macromolecular crowding may shift the equilibria for actin polymerization and modulate the rates of bundle assembly. Then,

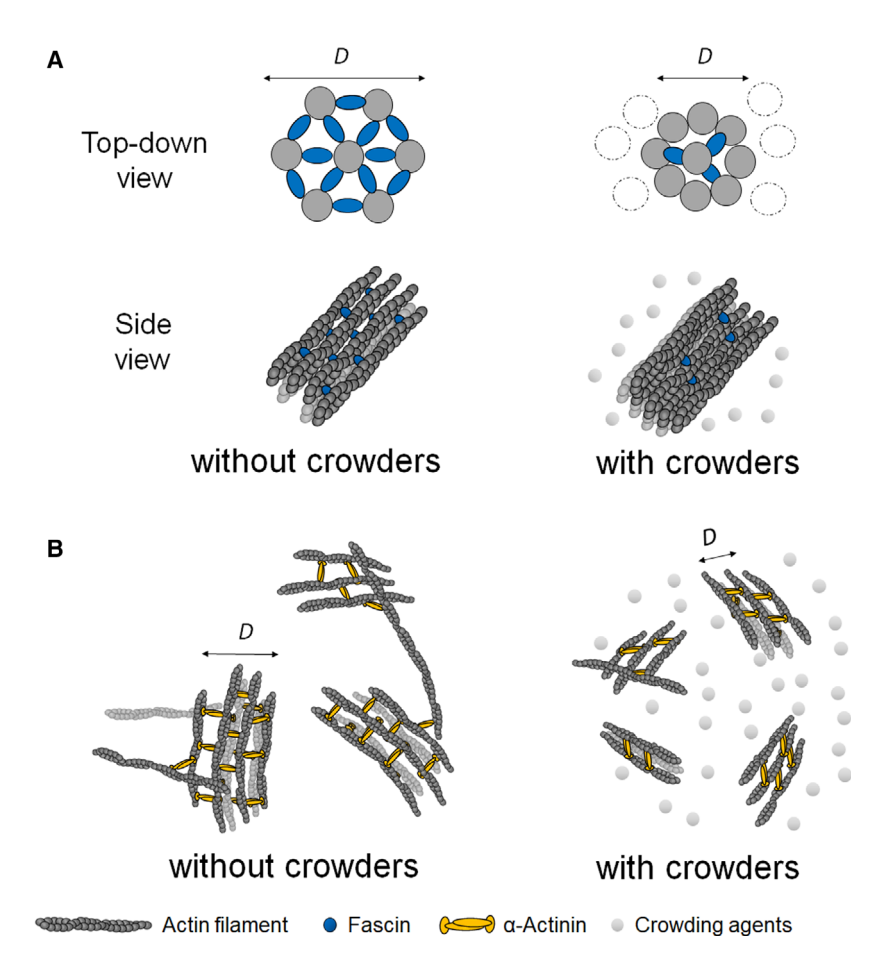


Fig. 6. Proposed scheme of bundling behavior of fascin and α -actinin in crowded condition. (A) Crowding induces densely packed fascin-induced bundles with increased number of filaments per bundle and decreased bundle diameter (D). Binding of fascin to actin filaments is reduced in crowded conditions. (B) Crowding reduces the binding of α -actinin to actin filaments, potentially leading to the formation of short and thin bundles. The diameter (D) and the number of filaments per bundle of α -actinincrosslinked bundles decrease in the presence of crowders. Crowded conditions may decrease the angle between α -actinin and filaments.

how would changes in actin polymerization kinetics play a role in modulating bundle organization? Falzone et al. [50] demonstrated production of alpha-actinin-induced bundle formation was possible through the presence of a fluid-like environment. The dilute solution enables F-actin to be highly mobile and thus able to dramatically increase the rate of bundle and network formation. When the distance between actin filaments is shorter than the filament length, the impaired filaments can result in a viscoelastic microenvironment upon crosslinking [50]. Changes of actin filament lengths modulate the elasticity of crosslinked actin networks [85]. Macromolecular crowding reduces average filament lengths [49] and enhances the elastic modulus of bundles and networks [86]. Therefore, the depletion forces induced by crowding may result in reductions in filament lengths and distance between filaments that can tune bundle thickness, along with modulations in elastic properties of cross-linked bundles and networks.

It is important to understand how fascin or α -actinin and depletion forces, either cooperatively or competitively, modulate actin bundle formation and mechanics, because crowding effects exist by default inside the cytoplasm. Depletion forces can bundle filaments without any crosslinkers by overcoming the electrostatic repulsion between filaments that are negatively charged [46]. On the other hand, bundles formed by crosslinking proteins depend on their binding affinity and on- and off-rates [24,47]. Reduced binding of fascin and α-actinin to actin filaments in the presence of crowding suggests that crowders can function as competitive agents for crosslinking proteins in actin bundle formation. This study motivates future experiments that examine the effects of crowding on bundling activities at varying concentrations of crosslinking proteins. Based on our data, we expect that the onset concentration of crosslinking proteins for bundling may shift (increase) with increasing concentration of crowders. Our findings also suggest that it is important to carefully evaluate possible changes in ABPs' activities and/or binding interactions with actin filaments when working with crowding agents in vitro. This work proposes the mechanisms of how the organization and mechanics of crosslinked actin bundles are modulated in crowded intracellular environments, which can advance our understanding of regulatory protein-induced bundling in vivo.

Acknowledgements

We thank anonymous reviewers for their insights and critical evaluation of the manuscript. Research reported

in this publication was supported by by the National Institute of Allergy and Infectious Diseases of the National Institutes of Health under Award Number R01AI139242 and funds from the University of Central Florida (UCF) awarded to E.H.K., and by the National Science Foundation award 1847830 awarded to L.T. The content is solely the responsibility of the authors and does not necessarily represent the official views of the National Institutes of Health. The authors acknowledge the computational resources from UCF STOKES cluster and resources of the National Energy Research Scientific Computing Center, a DOE Office of Science User Facility supported by the Office of Science of the U.S. Department of Energy under Contract No. DE-AC02-05CH11231. We gratefully acknowledge Kang group members for their continued support and UCF Nanoscience Technology Center as well as the Biomolecular Research Annex for shared equipment.

Author contributions

J.P., M.L., and E.H.K. designed research; J.P., B.L., and N.C. performed experiments; M.L. performed MD simulations; J.P., M.L., B.L., and N.C. analyzed data; J.P., M.L., B.L., N.C., L.T., and E.H.K. wrote and revised the paper.

References

- 1 Chhabra ES and Higgs HN (2007) The many faces of actin: matching assembly factors with cellular structures. *Nat Cell Biol* 9, 1110–1121.
- 2 Fletcher DA and Mullins RD (2010) Cell mechanics and the cytoskeleton. *Nature* **463**, 485–492.
- 3 Blanchoin L, Boujemaa-Paterski R, Sykes C and Plastino J (2014) Actin dynamics, architecture, and mechanics in cell motility. *Physiol Rev* **94**, 235–263.
- 4 Pollard TD and Cooper JA (2009) Actin, a central player in cell shape and movement. *Science* **326**, 1208–1212.
- 5 Colombelli J, Besser A, Kress H, Reynaud EG, Girard P, Caussinus E, Haselmann U, Small JV, Scharz US and Stelzer EH (2009) Mechanosensing in actin stress fibers revealed by a close correlation between force and protein localization. *J Cell Sci* **122**, 1665–1679.
- 6 Burridge K and Wittchen ES (2013) The tension mounts: Stress fibers as force-generating mechanotransducers. *J Cell Biol* **200**, 9–19.
- 7 Luo T, Mohan K, Iglesias PA and Robinson DN (2013) Molecular mechanisms of cellular mechanosensing. *Nat Mater* 12, 1064–1071.
- 8 Rückerl F, Lenz M, Betz T, Manzi J, Martiel JL, Safouane M, Parterski-Boujemaa R, Blanchoin L and Sykes C (2017) Adaptive response of actin bundles under mechanical stress. *Biophys J* **113**, 1072–1079.

- 9 Nemethova M, Auinger S and Small JV (2008) Building the actin cytoskeleton: filopodia contribute to the construction of contractile bundles in the lamella. *J Cell Biol* **180**, 1233–1244.
- 10 Svitkina TM, Bulanova EA, Chaga OY, Vignjevic DM, Kojima S-I, Vasiliev JM and Borisy GG (2003) Mechanism of filopodia initiation by reorganization of a dendritic network. *J Cell Biol* 160, 409–421.
- 11 Khurana S and George SP (2011) The role of actin bundling proteins in the assembly of filopodia in epithelial cells. *Cell Adh Migr* **5**, 409–420.
- 12 Dobramysl U, Papoian GA and Erban R (2016) Steric effects induce geometric remodeling of actin bundles in filopodia. *Biophys J* **110**, 2066–2075.
- 13 Tojkander S, Gateva G and Lappalainen P (2012) Actin stress fibers – assembly, dynamics and biological roles. *J Cell Sci* **125**, 1855–1864.
- 14 Naumanen P, Lappalainen P and Hotulainen P (2008) Mechanisms of actin stress fibre assembly. *J Microsc* 231, 446–454.
- 15 Narayanan P, Chatterton P, Ikeda A, Ikeda S, Corey DP, Ervasti JM and Perrin BJ (2015) Length regulation of mechanosensitive stereocilia depends on very slow actin dynamics and filament-severing proteins. *Nat Commun* 6, 6855.
- 16 Tilney LG, Connelly P, Smith S and Guild GM (1996) F-actin bundles in *Drosophila* bristles are assembled from modules composed of short filaments. *J Cell Biol* 135, 1291–1308.
- 17 Guild GM, Connelly PS, Ruggiero L, Vranich KA and Tilney LG (2003) Long continuous actin bundles in *Drosophila* bristles are constructed by overlapping short filaments. *J Cell Biol* **162**, 1069–1077.
- 18 Bathe M, Heussinger C, Claessens MMAE, Bausch AR and Frey E (2008) Cytoskeletal bundle mechanics. *Biophys J* **94**, 2955–2964.
- 19 Michelot A and Drubin DG (2011) Building distinct actin filament networks in a common cytoplasm. *Curr Biol* 21, R560–R569.
- 20 Claessens MMAE, Bathe M, Frey E and Bausch AR (2006) Actin-binding proteins sensitively mediate Factin bundle stiffness. *Nat Mater* 5, 748–753.
- 21 Bartles JR (2000) Parallel actin bundles and their multiple actin-bundling proteins. *Curr Opin Cell Biol* 12, 72–78.
- 22 Lieleg O, Claessens MMAE, Luan Y and Bausch AR (2008) Transient binding and dissipation in cross-linked actin networks. *Phys Rev Lett* 101, 108101.
- 23 Winkelman JD, Suarez C, Hocky GM, Harker AJ, Morganthaler AN, Christensen JR, Voth GA, Bartles JR and Kovar DR (2016) Fascin- and alpha-actininbundled networks contain intrinsic structural features that drive protein sorting. *Curr Biol* 26, 2697–2706.

- 24 Courson DS and Rock RS (2010) Actin cross-link assembly and disassembly mechanics for alpha-actinin and fascin. *J Biol Chem* **285**, 26350–26357.
- 25 Jansen S, Collins A, Yang C, Rebowski G, Svitkina T and Dominguez R (2011) Mechanism of actin filament bundling by fascin. *J Biol Chem* 286, 30087–30096.
- 26 Ono S, Yamakita Y, Yamashiro S, Matsudaira PT, Gnarra JR, Obinata T and Matsumura F (1997) Identification of an actin binding region and a protein kinase C phosphorylation site on human fascin. *J Biol Chem* 272, 2527–2533.
- 27 Kureishy N, Sapountzi V, Prag S, Anilkumar N and Adams JC (2002) Fascins, and their roles in cell structure and function. *BioEssays* 24, 350–361.
- 28 Vignjevic D, Kojima S, Aratyn Y, Danciu O, Svitkina T and Borisy GG (2006) Role of fascin in filopodial protrusion. *J Cell Biol* **174**, 863–875.
- 29 Adams JC (2004) Roles of fascin in cell adhesion and motility. Curr Opin Cell Biol 16, 590–596.
- 30 Mattila PK and Lappalainen P (2008) Filopodia: molecular architecture and cellular functions. *Nat Rev Mol Cell Biol* 9, 446–454.
- 31 Takatsuki H, Bengtsson E and Månsson A (2014)
 Persistence length of fascin-cross-linked actin filament bundles in solution and the in vitro motility assay. *Biochim Biophys Acta* **1840**, 1933–1942.
- 32 Ribeiro EA, Pinotsis N, Ghisleni A, Salmazo A, Konarev PV, Kostan J, Sjöblom B, Schreiner C, Polyansky AA, Gkougkoulia EA *et al.* (2014) The structure and regulation of human muscle α-actinin. *Cell* **159**, 1447–1460.
- 33 Tang J, Taylor DW and Taylor KA (2001) The three-dimensional structure of alpha-actinin obtained by cryoelectron microscopy suggests a model for Ca (2+)-dependent actin binding. *J Mol Biol* **310**, 845–858.
- 34 Xue F, Janzen DM and Knecht DA (2010) Contribution of filopodia to cell migration: a mechanical link between protrusion and contraction. *Int* J Cell Biol 2010, 507821.
- 35 Sjöblom B, Salmazo A and Djinović-Carugo K (2008) α-Actinin structure and regulation. *Cell Mol Life Sci* **65**, 2688–2701.
- 36 Meyer RK and Aebi U (1990) Bundling of actin filaments by alpha-actinin depends on its molecular length. J Cell Biol 110, 2013–2024.
- 37 Wachsstock DH, Schwartz WH and Pollard TD (1993) Affinity of alpha-actinin for actin determines the structure and mechanical properties of actin filament gels. *Biophys J* **65**, 205–214.
- 38 Strehle D, Schnauss J, Heussinger C, Alvarado J, Bathe M, Kas J and Gentry B (2011) Transiently crosslinked F-actin bundles. Eur Biophys J 40, 93–101.

- 39 Ellis RJ (2001) Macromolecular crowding: obvious but underappreciated. Trends Biochem Sci 26, 597–604.
- 40 Frederick KB, Sept D and De La Cruz EM (2008) Effects of solution crowding on actin polymerization reveal the energetic basis for nucleotide-dependent filament stability. *J Mol Biol* 378, 540–550.
- 41 Gao M and Winter R (2015) Kinetic insights into the elongation reaction of actin filaments as a function of temperature, pressure, and macromolecular crowding. *Chem Phys Chem* **16**, 3681–3686.
- 42 Rashid R, Chee SML, Raghunath M and Wohland T (2015) Macromolecular crowding gives rise to microviscosity, anomalous diffusion and accelerated actin polymerization. *Phys Biol* 12, 034001.
- 43 Rosin C, Esterl K, Hälker J and Winter R (2015) Combined effects of temperature, pressure, and cosolvents on the polymerization kinetics of actin. *Chem Phys Chem* **16**, 1379–1385.
- 44 Lindner RA and Ralston GB (1997) Macromolecular crowding: effects on actin polymerisation. *Biophys Chem* **66**, 57–66.
- 45 Drenckhahn D and Pollard TD (1986) Elongation of actin filaments is a diffusion-limited reaction at the barbed end and is accelerated by inert macromolecules. *J Biol Chem* 261, 12754–12758.
- 46 Hosek M and Tang JX (2004) Polymer-induced bundling of F-actin and the depletion force. *Phys Rev E* **69**, 051907.
- 47 Schnauß J, Händler T and Käs J (2016) Semiflexible biopolymers in bundled arrangements. *Polymers* **8**, 274.
- 48 Huber F, Strehle D and Käs J (2012) Counterioninduced formation of regular actin bundle networks. *Soft Matter* **8**, 931–936.
- 49 Castaneda N, Lee M, Rivera-Jacquez HJ, Marracino RR, Merlino TR and Kang H (2019) Actin filament mechanics and structure in crowded environments. *J Phys Chem B* 123, 2770–2779.
- 50 Falzone TT, Lenz M, Kovar DR and Gardel ML (2012) Assembly kinetics determine the architecture of α-actinin crosslinked F-actin networks. *Nat Commun* **3**, 861.
- 51 Untracht ZT, Ozcan A, Santra S and Kang EH (2020) SDS-PAGE for monitoring the dissolution of zinc oxide bactericidal nanoparticles (zinkicide) in aqueous solutions. *ACS Omega* **5**, 1402–1407.
- 52 Castaneda N, Zheng T, Rivera-Jacquez HJ, Lee HJ, Hyun J, Balaeff A, Huo Q and Kang H (2018) Cations modulate actin bundle mechanics, assembly dynamics, and structure. J Phys Chem B 122, 3826–3835.
- 53 Breitsprecher D, Koestler SA, Chizhov I, Nemethova M, Mueller J, Goode BL, Small JV, Rottner K and Faix J (2011) Cofilin cooperates with fascin to disassemble filopodial actin filaments. *J Cell Sci* 124, 3305–3318.
- 54 Graham JS, McCullough BR, Kang H, Elam WA, Cao W and De La Cruz EM (2014) Multi-platform

- compatible software for analysis of polymer bending mechanics. *PLoS One* **9**, e94766.
- 55 Gittes F, Mickey B, Nettleton J and Howard J (1993) Flexural rigidity of microtubules and actin filaments measured from thermal fluctuations in shape. *J Cell Biol* 120, 923–934.
- 56 Lee B, Castaneda N, Doomra M, Modha N, Santra S, Thornton J, Zhang T, Kang EH and Tetard L (2020) Nanoscale quantification of longitudinal and transverse mechanics of bacterial bodies. *Appl Phys Lett* 116, 053701.
- 57 Diaz AM, Zhang Z, Lee B, Luna FMH, Li Sip YY, Lu X, Heidings J, Tetard L, Zhai L and Kang H (2018) Evaluation of single hydrogel nanofiber mechanics using persistence length analysis. *ACS Omega* 3, 18304–18310.
- 58 Lyubchenko YL (2011) Preparation of DNA and nucleoprotein samples for AFM imaging. *Micron* 42, 196–206.
- 59 Liu Z, Li Z, Zhou H, Wei G, Song Y and Wang L (2005) Imaging DNA molecules on mica surface by atomic force microscopy in air and in liquid. *Microsc Res Techniq* 66, 179–185.
- 60 Nečas D and Klapetek P (2012) Gwyddion: an opensource software for SPM data analysis. *Open Phys* 10, 181–188.
- 61 Galkin VE, Orlova A, Vos MR, Schröder GF and Egelman EH (2015) Near-atomic resolution for one state of F-actin. *Structure* **23**, 173–182.
- 62 Shams H, Golji J, Garakani K and Mofrad MRK (2016) Dynamic regulation of α-actinin's calponin homology domains on F-actin. *Biophys J* 110, 1444–1455.
- 63 Galkin VE, Orlova A, Salmazo A, Djinovic-Carugo K and Egelman EH (2010) Opening of tandem calponin homology domains regulates their affinity for F-actin. *Nat Struct Mol Biol* 17, 614–616.
- 64 Pierce BG, Wiehe K, Hwang H, Kim BH, Vreven T and Weng Z (2014) ZDOCK server: interactive docking prediction of protein-protein complexes and symmetric multimers. *Bioinformatics* **30**, 1771–1773.
- 65 Yang S, Huang FK, Huang K, Chen S, Jakoncic J, Leo-Macias A, Diaz-Avalos R, Chen L, Zhang JJ and Huang XY (2013) Molecular mechanism of fascin function in filopodial formation. *J Biol Chem* 288, 274–284.
- 66 Galkin VE, Orlova A, Schroder GF and Egelman EH (2010) Structural polymorphism in F-actin. *Nat Struct Mol Biol* 17, 1318–1323.
- 67 Martinez L, Andrade R, Birgin EG and Martinez JM (2009) PACKMOL: a package for building initial configurations for molecular dynamics simulations. J Comput Chem 30, 2157–2164.
- 68 Phillips JC, Braun R, Wang W, Gumbart J, Tajkhorshid E, Villa E, Chipot C, Skeel RD, Kalé L

- and Schulten K (2005) Scalable molecular dynamics with NAMD. *J Comput Chem* **26**, 1781–1802.
- 69 Vorobyov I, Anisimov VM, Greene S, Venable RM, Moser A, Pastor RW and MacKerell AD (2007) Additive and classical drude polarizable force fields for linear and cyclic ethers. *J Chem Theory Comput* 3, 1120–1133.
- 70 Vanommeslaeghe K, Hatcher E, Acharya C, Kundu S, Zhong S, Shim J, Darian E, Guvench O, Lopes P, Vorobryov I et al. (2010) CHARMM general force field: a force field for drug-like molecules compatible with the CHARMM all-atom additive biological force fields. J Comput Chem 31, 671–690.
- 71 Guvench O, Mallajosyula SS, Raman EP, Hatcher E, Vanommeslaeghe K, Foster TJ, Jamison FW II and Mackerell AD Jr (2011) CHARMM additive all-atom force field for carbohydrate derivatives and its utility in polysaccharide and carbohydrate-protein modeling. *J* Chem Theory Comput 7, 3162–3180.
- 72 Humphrey W, Dalke A and Schulten K (1996) VMD: visual molecular dynamics. *J Mol Graph* **14**, 33–38.
- 73 Ghosh S, Park J, Thomas M, Cruz E, Cardona O, Kang H and Jewett T (2018) Biophysical characterization of actin bundles generated by the *Chlamydia trachomatis* tarp effector. *Biochem Biophy Res Commun* **500**, 423–428.
- 74 Luckham PF and Klein J (1984) Forces between mica surfaces bearing adsorbed polyelectrolyte, poly-L-lysine, in aqueous media. J Chem Soc Faraday Trans 80, 865–878.
- 75 Kuznetsova IM, Turoverov KK and Uversky VN (2014) What macromolecular crowding can do to a protein. *Int J Mol Sci* 15, 23090–23140.
- 76 Mardoum WM, Gorczyca SM, Regan KE, Wu T-C and Robertson-Anderson RM (2018) Crowding induces entropically-driven changes to DNA dynamics that depend on Crowder structure and ionic conditions. Front Phys 6, 53.
- 77 Kang H, Toan NM, Hyeon C and Thirumalai D (2015) Unexpected swelling of stiff DNA in a polydisperse crowded environment. *J Am Chem Soc* **137**, 10970–10978.
- 78 Pelletier O, Pokidysheva E, Hirst LS, Bouxsein N, Li Y and Safinya CR (2003) Structure of actin cross-linked with α-actinin: a network of bundles. *Phys Rev Lett* **91**, 148102.
- 79 Gilmore JL, Kumeta M and Takeyasu K (2013) AFM investigation of the organization of actin bundles formed by actin-binding proteins. J Surf Eng Mater Adv Technol 3, 13–19.

- 80 Haviv L, Gov N, Ideses Y and Bernheim-Groswasser A (2008) Thickness distribution of actin bundles in vitro. *Eur Biophys J* **37**, 447–454.
- 81 López CJ, Fleissner MR, Guo Z, Kusnetzow AK and Hubbell WL (2009) Osmolyte perturbation reveals conformational equilibria in spin-labeled proteins. *Protein Sci* 18, 1637–1652.
- 82 Gagarskaia IA, Povarova OI, Uversky VN, Kuznetsova IM and Turoverov KK (2017) The effects of crowding agents Dextran-70k and PEG-8k on actin structure and unfolding reaction. *J Mol Struct* **1140**, 46–51.
- 83 Guseman AJ, Goncalves GMP, Speer SL, Young GB and Pielak GJ (2018) Protein shape modulates crowding effects. *Proc Natl Acad Sci USA* 115, 10965–10970.
- 84 Goins AB, Sanabria H and Waxham MN (2008) Macromolecular crowding and size effects on probe microviscosity. *Biophys J* **95**, 5362–5373.
- 85 Kasza KE, Broedersz CP, Koenderink GH, Lin YC, Messner W, Millman EA, Nakamura F, Stossel TP, Mackintosh FC and Weitz DA (2010) Actin filament length tunes elasticity of flexibly cross-linked actin networks. *Biophys J* 99, 1091–1100.
- 86 Tharmann R, Claessens MMAE and Bausch AR (2006) Micro-and macrorheological properties of actin networks effectively cross-linked by depletion forces. *Biophys J* 90, 2622–2627.

Supporting information

Additional supporting information may be found online in the Supporting Information section at the end of the article.

- Fig. S1. Effects of crowding on F-actin alone.
- **Fig. S2.** Low-speed co-sedimentation assay of fascin-induced bundles without and with crowders.
- Fig. S3. Low-speed co-sedimentation assay of α -actinin-induced bundles without and with crowders.
- **Fig. S4.** Diameter distribution of actin bundles without and with crowders.
- Fig. S5. Calculated Young's modulus $(E_{\rm B})$ of fascin-induced bundles without and with crowders.
- **Fig. S6.** Radius of gyration (R_{α}) analysis.
- Fig. S7. Root mean square displacement (RMSD) analysis.
- **Fig. S8.** Interaction energy and inter-hydrogen bonds analysis.